Polymerization of Single-Wall Carbon Nanotubes under High Pressures and High Temperatures

Valery N. Khabashesku,* Zhenning Gu, Bruce Brinson, John L. Zimmerman, and John L. Margrave

Department of Chemistry, Rice Quantum Institute and Center for Nanoscale Science and Technology, Rice University, Houston, Texas 77005-1892

Valery A. Davydov, Lyudmila S. Kashevarova, and Alexandra V. Rakhmanina

Institute of High Pressure Physics of the Russian Academy of Sciences, Troitsk, Moscow Region, Russian Federation

Received: April 21, 2002; In Final Form: September 6, 2002

Survey studies of pressure−temperature-induced transformations of single-wall carbon nanotubes (SWNT) at 1.5, 8.0, and 9.5 GPa and temperatures ranging from 200 to 1500 °C in a piston-cylinder or "Toroid" type high pressure devices have been carried out. It was found that the combined effects of high pressures and high temperatures produce irreversible changes in the SWNT structure, in contrast with the reversible effect of high pressure alone, previously studied by several research groups. The Raman, electron microscopy, and X-ray diffraction data obtained in the present work provide evidence for covalent interlinking of SWNT by sp^3 C−C bonds which escalates with the increasing treatment temperature and pressure. The formation of new carbon structures such as nano- and microcrystalline diamond-like (cubic and hexagonal) and nanographite phases under higher pressures (8.0 and 9.5 GPa) has been observed.

Introduction

Transformations of the atomic sp^2 hybridization states into the sp^3 states in carbon and heterocarbon materials, taking place in the course of their cross-linking polymerization, are considered as essential mechanistic steps to formation of high-density superhard phases. Graphite/diamond and h-BN/c-BN conversions can be given as classical examples.[1,2] However, the direct non-catalyzed cross-linking of plane graphene sheets in graphite to form cubic diamond normally requires very high pressures and temperatures (above 13 GPa and 3000 °C, respectively), which are quite difficult and costly to achieve.[3]

In the curved carbon nanostructures, e. g., fullerenes and nanotubes, C═C π-bonds are activated by partial pyramidalization of the sp^2 carbon configuration. This provides for a large number of reactive sites with increased p-orbital character which suggests that the cross-linking chemical interactions in nanocarbons to form covalent sp^3 C−C bonds can occur under milder conditions (pressure and temperature), more suitable for practical purposes. In this case, the use of curved carbon nanostructures as precursors for the high pressure-high temperature (HPHT) treatment unfolds wide opportunities for preparation of a variety of previously unknown carbon materials with unique properties. Thermodynamically, these new materials represent intermediate states being formed during pressure-induced transformation of the carbon system from a highly metastable states (fullerenes, nanotubes) to the equilibrium states (graphite and diamond).

The recent extensive studies[4−11] have demonstrated that the pressure-induced polymerization of fullerene C_{60} via 2+2 cycloaddition reactions take place already at room temperature under pressures above 1 GPa. Under these conditions the dimer $(C_{60})_2$ is formed as the main product. The increases of pressure (up to 8 GPa) and temperature (up to 700 °C) give rise to formation of more complex products, linear one-dimensional (1D) and two-dimensional (2D) tetragonal and trigonal C_{60} polymers. The three-dimensional (3D) C_{60} polymers are formed under HPHT treatment under pressures above 8 GPa. The molecular packing of the 1D and 2D polymers into individual crystalline phases have been described by orthorhombic (O), tetragonal (T), and rhombohedral (R) structural models.[5,6] Successful HPHT synthesis of practically pure single-phase samples of O, T, and R polymers of C_{60} allowed detailed investigation of their vibrational,[11] electrical,[12] and magnetic[13] properties, leading to the discovery of ferromagnetic behavior shown by the R phase.[13] The 3D polymerized C_{60} phases were found to be superhard, some of them with hardness comparable to that of diamond according to experimental and theoretical modeling data.[14−16]

Polymerization of single-wall carbon nanotubes (SWNT) was also theoretically predicted to proceed by analogy with fullerenes via 2+2 cycloaddition reactions producing covalently interlinked sp^3-bonded structures.[17,18] This process could be of significant importance for preparation of carbon nanofibers and nanocomposites with stronger mechanical properties than nanoropes in which the neighboring SWNT are held together only by van der Waals forces. Application of high pressure techniques to SWNT has already shown to be a powerful tool for varying the intertube distance.[19−24] However, the recent in situ Raman[21] and X-ray[23,24] studies done in a diamond anvil cell at ambient temperature under hydrostatic pressures up to 25.9 GPa[21] and 13 GPa,[24] respectively, have indicated that the high pressures alone are not likely to induce the covalent interlinking of SWNT. These nanotubes were always observed to recover from a

* Corresponding author. E-mail: khval@rice.edu.

10.1021/jp025983w CCC: $22.00
Published on Web 10/03/2002

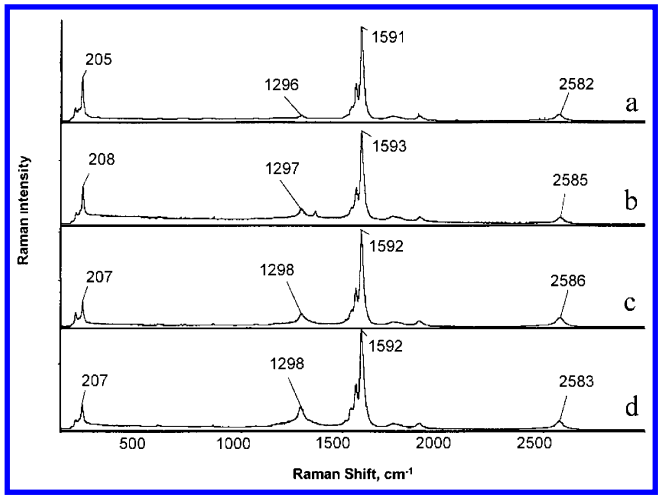

Figure 1. Raman spectra of pristine SWNT (a) and SWNT treated at 1.5 GPa and temperatures 300 °C (b), 500 °C (c), and 700 °C (d).

pressure-induced distorted shape to a circular shape on pressure release, thus confirming their predicted remarkable mechanical resilience.

Motivated by successful syntheses of single-phase samples of polymeric C_{60} under combined effects of high pressure and high temperature,[11] we have carried out a series of HPHT experiments on SWNT. The results of this work have partially been presented at conferences.[25,26] The current paper provides a more detailed report on our studies of HPHT-induced transformations of SWNT toward covalently cross-linked carbon nanostructures.

Experimental Details

The experimental part of this work involved the following steps: (i) HPHT treatment of the SWNT in the pressure range up to 10 GPa and temperatures up to 1500 °C, (ii) quenching of the high pressure states formed down to room temperature under pressure applied, (iii) ex situ characterization of the isolated states by optical spectroscopy, electron microscopy, and X-ray diffraction techniques to obtain information on materials bulk and microstructure.

The SWNT used as precursors in the present HPHT studies have been prepared by a laser vaporization method[27,28] and purified according to an oxidizing acid reflux procedure.[29,30] Such produced and processed SWNTs were of about 1.2 nm average diameter and lengths in the range from 100 nm to 1−2 μm, containing only a trace amount of the Ni/Co metal catalyst after purification.

Prior to the HPHT treatment, the SWNT samples were pressed in a hardened steel dye to form a pellets (typically of 2.5 mm diameter and 2.5−3.5 mm thickness). The pellets were wrapped by thin tantalum foil and embedded in a boron nitride cylinder meant to protect the samples from the graphite heater. Thereafter, the samples have been transferred into a chamber of "Maxim" (a piston-cylinder type) or "Toroid"[31] high pressure devices. The experimental procedure consisted in loading the samples up to the required pressure (1.5, 8.0, and 9.5 GPa) at room temperature, followed by their heating and isothermal holding at temperatures (from 200 to 1500 °C) and variable exposure times (from 5 to 300 s) under constant load. The temperature measurements were taken directly on the side surface of the sample by using chromel−alumel or platinum−platinum/rhodium thermocouples. The pressure in the reaction chamber was determined according to calibration curves. These

Figure 2. SEM images of pristine SWNT (a) and SWNT treated at 1.5 GPa and temperatures 300 °C (b), 500 °C (c), and 700 °C (d).

and the other aspects of the HPHT experiments have been described in more detail elsewhere.[31,32]

The high pressure states formed in the system were conserved by quenching them down to room temperature under pressure. Thereafter, they were studied at ambient conditions. The HPHT-treated samples, obtained as pellets, have been cut in half and characterized ex situ by micro-Raman spectroscopy, X-ray diffraction,and SEM/EDAX techniques followed in some cases by electron microprobe analysis (EPMA). Ground samples were

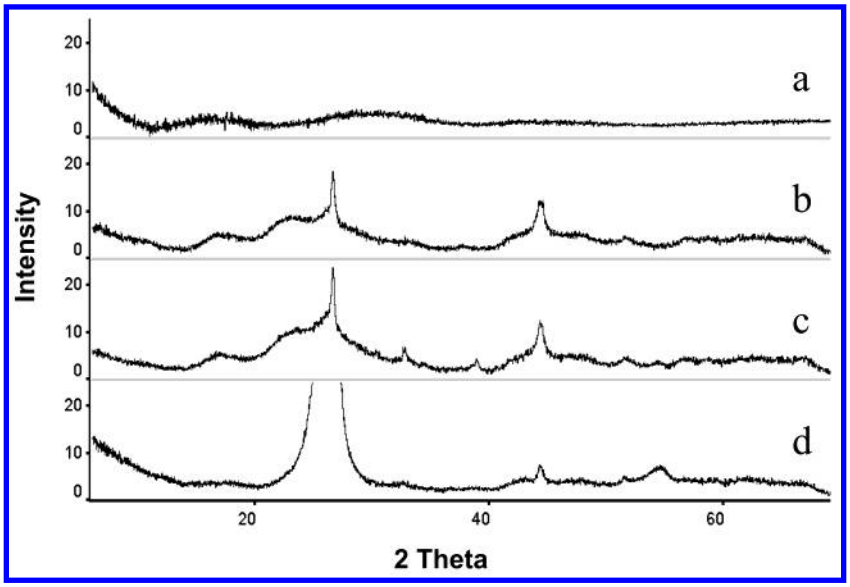

Figure 3. X-ray diffraction patterns for pristine SWNT (a) and SWNT treated at 1.5 GPa and temperatures 300 °C (b), 500 °C (c), and 700 °C (d). The intensity scale for each of traces (a−c) is expanded five times relative to trace (d).

studied by TEM/selected area diffraction (SAD) methods. Raman spectroscopy measurements for the samples placed on the top of a standard microscope slide were carried out on a Renishaw System 1000 micro-Raman spectrometer operating with an AlGaAs diode 780 nm laser. Scanning electron microscopy (SEM) was performed at 30 kV beam energy using a Phillips XL-30 field emission microscope equipped with an energy-dispersive X-ray (EDAX) analyzer. Transmission electron microscopy (TEM) photoimages of the specimen placed on lacey carbon-coated copper grids (size 200 mesh) were obtained with a JEOL JEM-2010 electron microscope operating at an accelerating voltage of 100 kV. X-ray diffraction data were collected on a GADDS powder diffractometer and a Rigaku D/MAX-2500H diffractometer with horizontal $\theta/2\theta$ goniometer equipped with a rotating anode as the Cu Kα radiation source. EPMA data were collected with the Cameca SX-50 electron microprobe analyzer equipped with PGT energy-dispersive spectrometer (EDS).

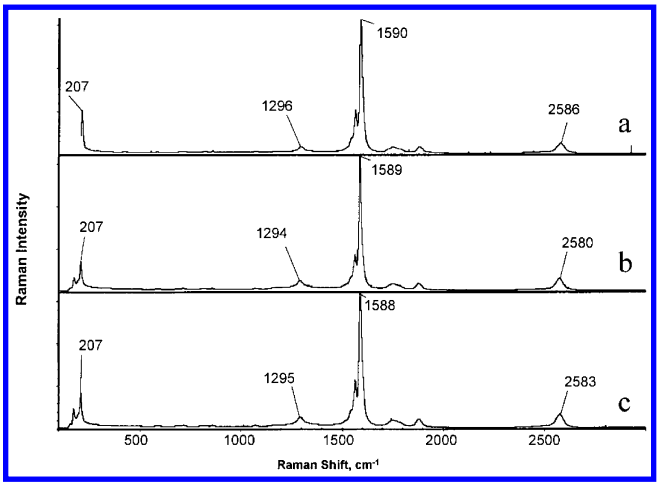

Figure 4. Raman spectra, taken for SWNT HPHT-treated at 1.5 GPa and temperatures 300 °C (a), 500 °C (b), 700 °C (c), after 2 h sonication in 2-propanol.

Results and Discussion

Survey characterization data collected by Raman, SEM, TEM/SAD and XRD methods for HPHT-treated SWNT under pressures of 1.5, 8.0, and 9.5 Gpa and temperatures 200−1500°C are shown in Figures 1−11. In these experiments the pressure of 1.5 GPa was chosen in view of both the demonstrated possibility of 1D and 2D polymerization for C_{60} under similar conditions[9] and recent theoretical and experimental data indicating that structural changes in the SWNT ropes start taking place under pressures as low as 1.5−1.7 GPa due to the faceting of neighboring tubes.[17,20,22,23] The effects of higher pressures (8.0 and 9.5 GPa) have also been studied because of the expected similarity in the behavior of SWNT with that of C_{60} fullerenes, which are shown to be transformed into highly cross-linked 3D phases by heating at ∼8−9 GPa and above.[11,14−16]

We have used Raman spectroscopy as the main tool for following the HPHT transformations of the SWNT, since over the last 30 years this technique has proven to be useful for examination of the sp^3 vs sp^2 types of bonding in carbon materials.[1,3] On Figure 1 the Raman spectrum of the pristine SWNT (a) is compared with the spectra of samples HPHT-treated at 1.5 GPa and 300 °C (b), 500 °C (c), and 700 °C (d). The dominant peaks near 205 cm^{-1} and around 1591 cm^{-1} in the first-order spectrum of the SWNT (Figure 1a) are universally considered to originate from radial breathing and tangential C−C bond stretching modes in nanotubes.[33] A very weak peak at 1296 cm^{-1} is normally related to the local defects, which originate from structural imperfections in the "as prepared" nanotubes and could be also contributed by the sp^3 carbons carrying residual −O− groups after the purification procedure.[29,30] The HPHT treatment of the SWNT causes a notable growth of the peak intensity at 1298 cm^{-1} and weakening of the peak at 207 cm^{-1} in the Raman spectra (Figure 1b−d) with the temperature increase. The SEM images of the samples, shown in Figure 2, demonstrate transformations of the pristine tangled SWNT bundles (a) to form thickened and aligned nanoropes (b, c), and nanoscale size plates (d) under treatment at the same pressure (1.5 GPa) and temperatures of 300 °C (b), 500 °C (c), and 700 °C (d), respectively. The image, shown in Figure 2d, particularly resembles those previously observed for the O- and T-phases of the HPHT-polymerized C_{60} under similar conditions.[9,11] Pristine SWNTs, used in the present work, did not exhibit any peaks in the XRD (Figure 3a), while the HPHT-treated samples show distinct patterns (Figure 3b−d). Two peaks, observed at 26.6° and 44.4° (2Θ) for the sample treated

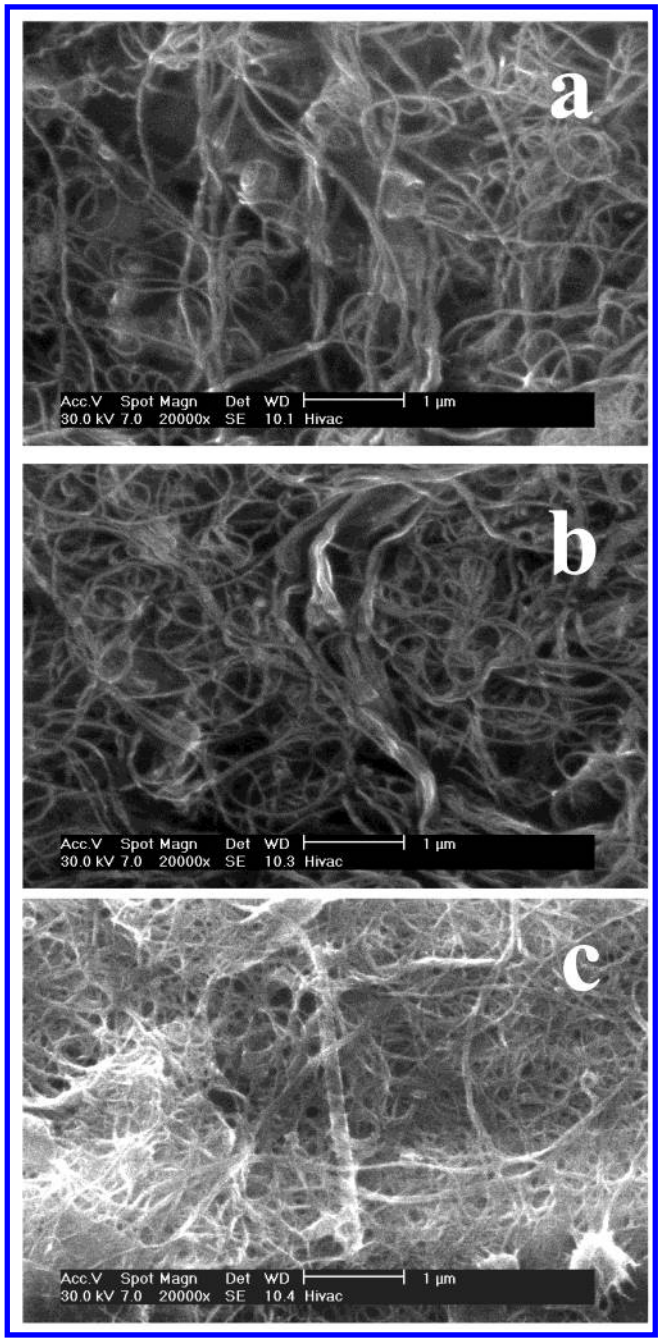

Figure 5. SEM images, obtained after 2 h sonication in 2-propanol of SWNT HPHT-treated at 1.5 GPa and temperatures 300 °C (a), 500 °C (b), 700 °C (c).

at 300 °C (Figure 3b), both gained intensity along with the appearance of additional peaks at 32.8°, 38.8°, 51.9°, and 54.6° (2Θ) in the XRD of the sample treated at 500 °C (Figure 3c), while treatment at 700 °C caused the intensity of the peak at 26.6° (2Θ) to increase five times with respect to other peaks (Figure 3d).

The changes observed in Raman, SEM, and XRD characteristics of SWNT samples under HPHT treatment can be explained by the covalent cross-linking of nanotube graphene walls occurring by formation of sp^3 C−C bonds, similar to the HPHT-induced 2+2 cycloaddition−polymerization of the C_{60} molecules. Depending on temperature- and pressure-assisted orientation of the SWNT bundles, the cross-linking can likely proceed along partial or full lengths of the nanotubes, which are close-packed within their bundled hexagonal structure. Thus, instead of producing chains, as in case of HPHT polymerization

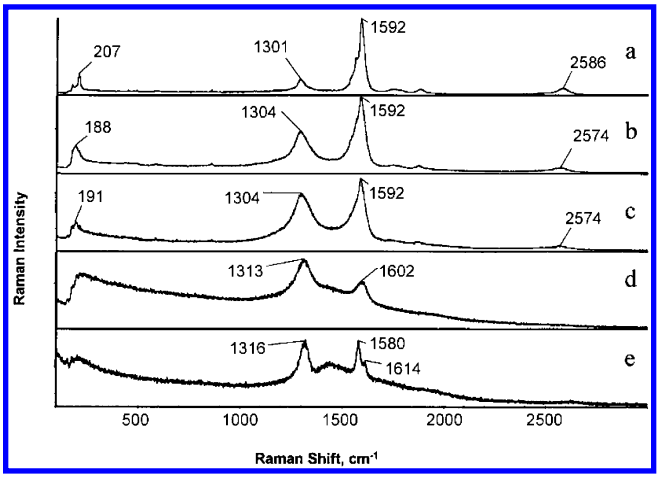

Figure 6. Raman spectra, taken for HPHT-treated SWNT at 8.0 GPa and temperatures 200 °C (a), 500 °C (b), 800 °C (c), 1200 °C (d), 1500 °C (e).

of C_{60} at 1.5 GPa, the cross-linked SWNTs are expected to assemble into raft-like planes.

The observed growth of intensity of the Raman peak at 1298 cm^{-1} with rising treatment temperature (Figure 1) definitely points at the increasing degree of sp^3 C−C bonding and densification of the material, which is clearly seen on the SEM micrographs (Figure 2). The morphology of the cross-linked SWNT-based materials, shown on these pictures, can probably be understood by taking into consideration the suggested faceting of the tubes under applied pressure, which changes the tube cross-section from circular to hexagonal or elliptical forming a honeycomb structure in the bundle. The faceting should result in a considerable overlapping of the flattened walls of neighboring tubes in the direction along their submicron-size length, closely resembling the stacking of graphene planes in graphite. The previous experiments, conducted without heating, have shown that these high pressure effects are reversible by demonstrating the restoration of the circular shape of the SWNT after decompression.

In our HPHT experiments the covalent C−C bonding of faceted tubes, taking place at the positions of their highest curvature points, prevents the tube from shape restoration and thus preserves the flat-wall profile of the SWNT monomer units in the newly formed carbon polymer structures isolated after quenching to ambient conditions. This also results in the lowering of the cylindrical symmetry of the tubes, which can help to explain the observed diminishing of the Raman intensity of the SWNT radial mode at 207 cm^{-1} (Figure 1a−d) with temperature increase. The graphite-like near-parallel stacking of the faceted and cross-linked tubes along their axes in these structures is evidenced by the appearance in their XRD (Figure 3) of the peak at 26.6° (2Θ) due to a graphitic interlayer *d* spacing (0.335 nm). Sharp growth of the intensity of this peak in the XRD of the sample prepared under the HPHT-treatment temperature of 700 °C (Figure 3d) correlates with the SEM data, showing thin plates (Figure 2d) which, due to more extensive SWNT cross-linking, are built from stacked planes of significantly larger area than in the case of covalently interlinked structures (Figure 2b,c) formed at lower temperatures.

Additional arguments for the high temperature-stimulated covalent cross-linking of SWNT under pressure of 1.5 GPa were obtained by observation of depolymerization of HPHT-treated samples. Sonication in 2-propanol for about 2 h at temperature 25−50 °C resulted in substantial degradation of their polymer structures and near complete recovery of initial SWNT bundles.

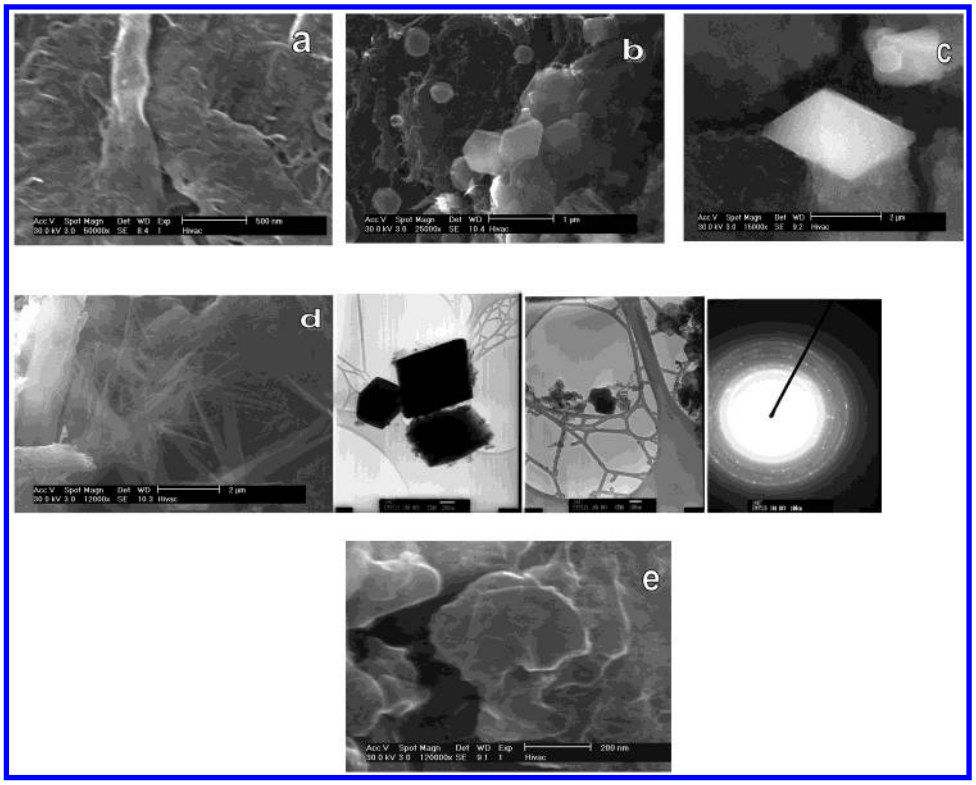

Figure 7. SEM images of HPHT-treated SWNT at 8.0 GPa and temperatures 200 °C (a), 500 °C (b), 800 °C (c), 1200 °C (d), 1500 °C (e). TEM images and SAD patterns are shown for the specimen prepared from the sample (d).

This is witnessed by notable reduction of the intensity of the peak at 1296 cm^{-1} in the Raman spectra (Figure 4) and by the observed similarity of the SEM images of sonicated samples (Figure 5) with those of pristine SWNTs (Figure 2a). Such a fairly easy depolymerization could be an indication of elongated and somewhat weakened intertube sp^3 C−C bonds in the HPHT materials produced at 1.5 GPa. This assumption agrees with the experimental and theoretical studies of the HPHT-polymerized C_{60} molecules, which show that the cross-linking sp^3 C−C bonds in the chainlike orthorhombic and layered tetragonal phases, prepared under the same pressure (1.5 GPa), are significantly longer (0.158−0.168 nm) than the C−C bonds in diamond (0.154 nm) and in the higher density hard carbon phases synthesized from C_{60} at higher pressures (6−13 GPa).

Depending on treatment temperatures, the HPHT transformations of SWNTs under higher pressure (8 GPa) resulted in an overall increase of the degree of sp^3 C−C cross-linking in the system. A comparison of the Raman spectra (Figure 6) and SEM images (Figure 7) of the HPHT-treated samples shows that with temperature increase from 200 to 1500 °C these materials gradually lose their nanotube structure and form entirely new all-carbon phases, which in some cases demonstrate a definite crystalline morphology, as confirmed by XRD and TEM/electron microdiffraction studies. The complete disappearance of SWNT features in the material takes place at temperatures above 800 °C, as evidenced by vanishing of the radial breathing mode in the Raman spectra (Figure 6d,e). The other observed changes in the Raman spectra (Figure 6) involved gradual growth of the intensity of the sp^3 carbon peak, which was found to be blue-shifted from 1301 to 1313 cm^{-1} on temperature increases from 200 to 1200 °C, respectively. These data likely indicate possibility of cross-linking in the material by shorter sp^3 C−C diamond-like bonds (0.154 nm) under the high pressure conditions studied (8 GPa), which corroborates the theoretical modeling of a two-dimensional polymerization of the SWNT.[18] The yield of these polymerized phases sharply increases with the temperature, therefore, on the SEM images in addition to one-dimensionally polymerized beam and raft-like structures (Figure 7a−c) polyhedral (hexagonal, cubic, and rhombohedral) nano- and micron-scale size crystallites (Figure 7b−d) were

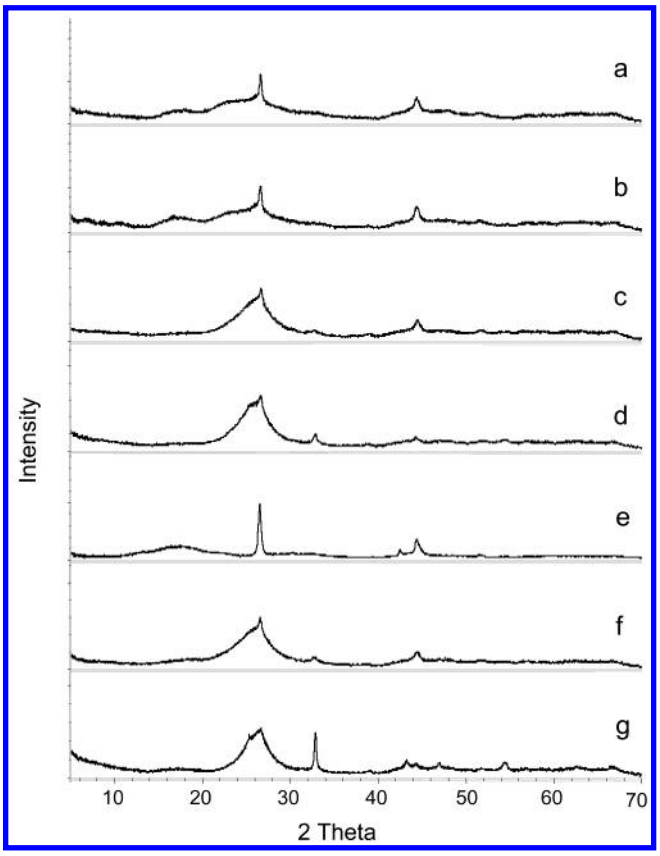

Figure 8. X-ray diffraction patterns for SWNT HPHT-treated at 8 GPa and temperatures 200 °C (a), 500 °C (b), 800 °C (c), 1200 °C (d), 1500 °C (e), as well as 9.5 GPa and 400 °C (f), and 600 °C (g).

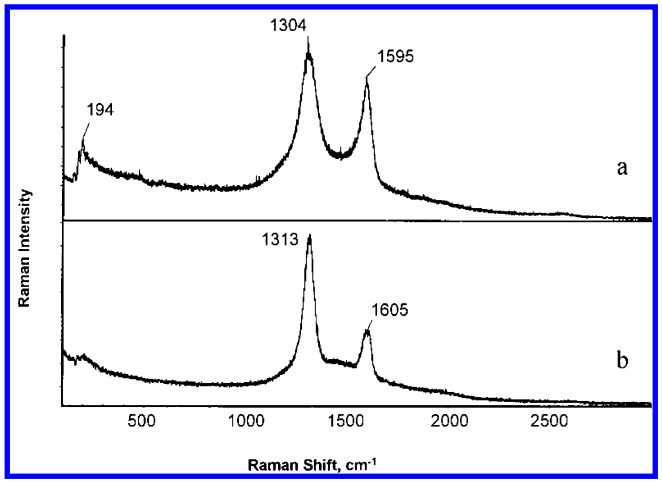

Figure 9. Raman spectra, taken for HPHT-treated SWNT at 9.5 GPa and temperatures 400 °C (a), and 600 °C (b).

observed to emerge. The electron microdiffraction patterns, such as the one obtained for the nanoscale-size particles shown in the TEM dark field images (Figure 7d), provide additional confirmation of the polycrystalline structure of these materials. This transformation probably also accounts for the appearance of new features in the XRD, such as the broad shoulder peak at 25.9° (2Θ) and the sharp peak at 32.8° (2Θ), at treatment temperatures of 800 and 1200 °C (Figure 8c,d).

Finally, the temperature increase to 1500 °C resulted in the predominant formation of a graphite phase, whose Raman spectrum (Figure 6e) was found to be identical with that of an authentic highly oriented pyrolytic graphite (HOPG) photoexcited with the same photon energy (780 nm). The observed X-ray diffraction patterns (Figure 8e) closely resembled those of HOPG. On the basis of the breadth of the (002) peak, the average particle size of the graphite phase was estimated to be 110 nm. The layered morphology of this HPHT-produced nanographite material has also been imaged by the SEM (Figure 7e). The formation of nanographite can be reasonably compared with the graphitization of nanodiamond powders, that was recently found to begin to occur on annealing in argon for 1 h at lower temperatures (above 800 °C) than in the case of bulk diamond (about 1500 °C).[34] In our experiments the use of high pressure (8 GPa) and high temperature prompted the production of highly crystalline graphite nanoparticles during a much shorter time (5 s). Under these conditions the nanographite is most likely formed by a multistep mechanism, which involves subsequent one- and two-dimensional polymerizations of faceted SWNTs into a nanosize diamond-like structures prior to their graphitization.

The HPHT treatment of SWNTs, carried out under the highest pressure applied in the present work (9.5 GPa), resulted in formation of highly polymerized crystalline carbon phases at a significantly lower temperature, as compared to the experiments done under pressure of 8 GPa. For instance, the XRD patterns of the sample obtained by treatment at 9.5 GPa and 400 °C (Figure 8f) show features similar to those for the material prepared at 8 GPa and 800 °C (Figure 8c). The same conclusion can be made about their corresponding Raman spectra, shown in Figures 9a and 6c. Both spectra exhibit a high-intensity broad peak at 1304 cm^{-1} due to the sp^3 C−C bonds. The presence of similarly shifted and weak nanotube features in both spectra should be particularly noted.Under pressure of 9.5 GPa the temperature increase to 600 °C already causes complete disappearance of nanotube modes in the Raman spectra (Figure 9b), while for samples treated at 8 Gpa it required temperatures as high as 1200 °C (Figure 6d). In addition, the 9.5 GPa sample shows the highest Raman intensity of the sp^3 C−C mode at 1313 cm^{-1} (Figure 9b), likely due to the presence of a small particle size diamond-like phase, and more prominent new peaks in the XRD (Figure 8g) at 25.2, 25.9, 32.8, 43.2, 47.0, 54.5° (2Θ) than in case of 8 GPa-treated sample (Figure 8d).

The SEM images taken on samples treated at 9.5 GPa revealed the occurrence of well-faceted nano- (Figure 10a,b) and micron-size (Figure 10c,d) crystallites which, according to EDAX and electron microprobe analyses, are all-carbon. The sample with the apparently highest content of these diamond-like crystals, obtained under treatment at 9.5 GPa and 600 °C, was more extensively studied by the TEM/SAD technique. The microdiffraction patterns of selected TEM specimens obtained are shown in Figure 11a−d. They provide evidence for

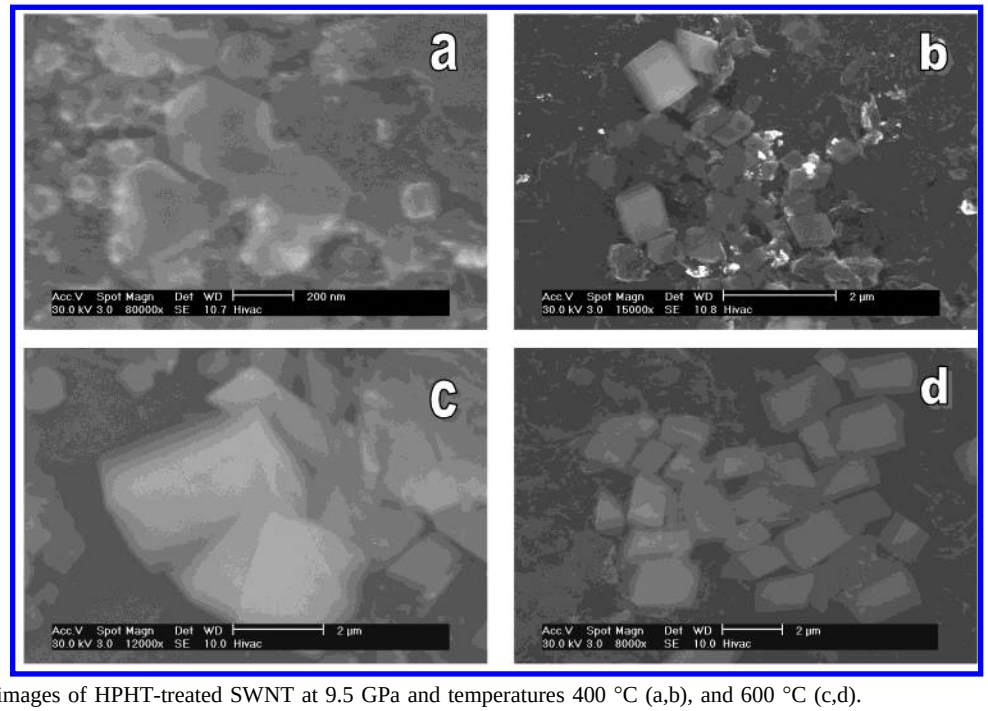

Figure 10. SEM images of HPHT-treated SWNT at 9.5 GPa and temperatures 400 °C (a,b), and 600 °C (c,d).

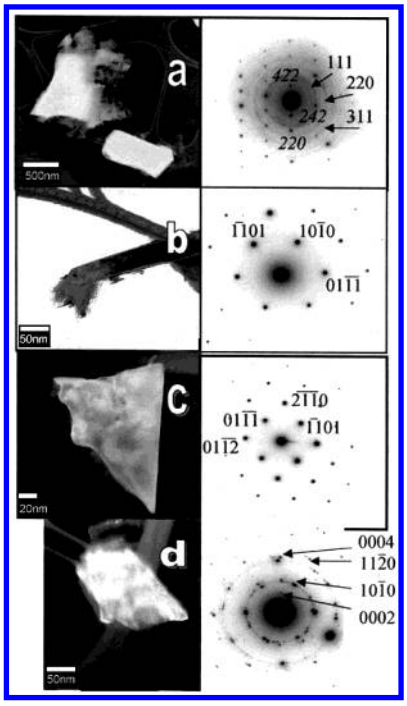

Figure 11. TEM images and corresponding SAD patterns for the specimen prepared from the sample of SWNT HPHT-treated at 9.5 GPa and 600 °C. Zone axes directions are shown in brackets. Diamond-like cubic phases, [113] direction for point pattern (a), and hexagonal (b), [113], (c), [0111], and (d) phases.

polycrystalline and single-crystalline cubic phases (Figure 11a) as well as several phases with a hexagonal structure (Figure 11b−d). From the electron diffraction ring patterns of the crystals, shown in Figure 11a and being similar to those observed by SEM (Figure 10d), a lattice constant ($a = 8.8$ Å) was calculated for their diamond-like cubic unit cell. Slightly larger cubic cell parameter ($a = 9.0$ Å) was derived from the overlapping point pattern detected for the same crystallite (Figure 11a). The larger size unit cells than in cubic diamond itself ($a = 3.567$ Å)[1] are likely due to the substantial presence of the sp^2-bonded carbons in the structures, which is evidenced by the observed peak at 1605 cm^{-1} in the micro-Raman spectrum of the material (Figure 9b). The hexagonal unit cell with the constants $a = 2.9$ Å, and $c = 5.15$ Å was suggested for the polyhedral rod-shaped crystallites, shown in Figure 11b, based on d spacings measured from their SAD patterns. Likewise, for the other phases observed by TEM, hexagonal unit cells with the estimated lattice parameters $a = 4.9$ Å, $c = 9.25$ Å (Figure 11c) and $a = 2.62$ Å, $c = 6.53$ Å (Figure 11d), respectively, were proposed. It is interesting to note that the a value for the phase, shown in Figure 11d, is found to be close to that in hexagonal diamond ($a = 2.52$ Å), which is known to form occasionally during HPHT synthesis.[1] The observed diversity of unit cell sizes in the phases prepared by the HPHT treatment of the SWNT is very likely related to a nanotube diameter distribution, ranging from 1.05 to 1.50 nm in the pristine SWNT.[30]

In conclusion, the obtained experimental data overall show that the transformations of SWNTs under pressures of 1.5−9.5 GPa and temperatures 200−1500°C are irreversible. We have presented spectroscopic evidence for covalent interlinking of SWNT by sp^3 C−C bonds and observed the formation of new carbon structures which included nano- and microcrystalline diamond-like (cubic and hexagonal) and nanographite phases being formed under higher pressures. The new diamond-like phases prepared from SWNT are expected to be very hard. This expectation is being further encouraged by the recent reports[35,36] of the synthesis of a 20 μm-thick film of super hard carbon material from SWNT by applying a shear deformation at a pressure of 24 GPa in a diamond anvil cell. The preparation of larger size samples of HPHT-polymerized SWNT are obviously required for precise characterization and structure/property relationship studies. This work is in progress in our laboratories.

Acknowledgment. The financial support from Texas Advanced Technology Program and The Robert Welch Foundation of Texas is especially appreciated. This work was also supported by the Russian Foundation for Basic Research, Grant No. 00-03-32600, and INTAS-RFBR program, Grant No. IR-97-1015. The authors thank C. Huffman and Professor R. Smalley for supplying the SWNT, R. Shukla for assistance in Raman and XRD samples characterization, and Dr. M. Pontier Johnson, Dr. R. H. Hauge, Professor E. N. Yakovlev, and Professor S. Stemmer for helpful discussions.

References and Notes

(1) *Handbook of Carbon, Graphite, Diamond and Fullerenes. Properties, Processing and Applications*; Pierson, H. O., Ed.; Noyes Publications: Park Ridge, New Jersey, 1993.

(2) *Properties of Group III Nitrides*; Edgar, J. H., Ed.; INSPEC, IEE Publ.: London, U.K., 1994.

(3) Bundy, F. P.; Strong, H. M.; Wentorf, R. H., Jr. *Chemistry and Physics of Carbon*, Vol. 10; Walker, P. L., Jr., Thrower, P. A., Eds.; Marcel Dekker Inc.: New York, 1973.

(4) Rao, A. M.; Zhou, R.; Wang, K. A.; Hager, G. T.; Holden, J. M.; Wang, Y.; Lee, W. T.; Be, X.-X.; Eklund, P. C.; Cornett, D. S.; Duncan, M. A.; Amster, I. J. *Science* **1993**, *259*, 955.

(5) Iwasa, Y.; Arima, T.; Fleming, R. M.; Siegrist, T.; Zhou, O.; Haddon, R. C.; Rothberg, L. J.; Lyons, K. B.; Carter, H. L., Jr.; Hebard, A. F.; Tycko, R.; Dabbagh, G.; Krajewski, J. L.; Thomas, G. A.; Yagi, T. *Science* **1994**, *264*, 1570.

(6) Nuñez-Regueiro, M.; Marques, L.; Hodeau, J.-L.; Berthoux, O.; Perroux, M. *Phys. Rev. Lett.* **1995**, *74*, 278.

(7) Eklund, P. C.; Rao, A. M.; Zhou, P.; Wang, Y.; Holden, J. M. *Thin Solid Films* **1995**, *257*, 185.

(8) Sundqvist, B. *Adv. Phys.* **1999**, *48*, 1.

(9) Davydov, V. A.; Kashevarova, L. S.; Rakhmanina, A. V.; Agafonov, V. A.; Allouchi, H.; Ceolin, R.; Dzyabchenko, A. V.; Senyavin, V. M.; Szwarc, H.; Tanaka, T.; Komatsu, K. *J. Phys. Chem. B* **1999**, *103*, 1800.

(10) Marques, L.; Mezouar, M.; Hodeau, J.-L.; Nuñez-Regueiro, M.; Serebryanaya, N. R.; Ivdenko, V. A.; Blank, V. D.; Dubitsky, G. A. *Science* **1999**, *283*, 1720, and references therein.

(11) Davydov, V. A.; Kashevarova, L. S.; Rakhmanina, A. V.; Senyavin, V. M.; Ceolin, R.; Szwarc, H.; Allouchi, H.; Agafonov, V. *Phys. Rev. B* **2000**, *61*, 11936.

(12) Makarova, T. L.; Sundqvist, B.; Scharff, P.; Gaevski, M. E.; Olsson, E.; Davydov, V. A.; Rakhmanina, A. V.; Kashevarova, L. S. *Carbon* **2001**, *39*, 2203.

(13) Makarova, T. L.; Sundqvist, B.; Höhne, R.; Esquinazi, P.; Kopelevich, Y.; Scharff, P.; Davydov, V. A.; Rakhmanina, A. V.; Kashevarova, L. S. *Nature* **2001**, *413*, 716.

(14) Blank, V. D.; Popov, M.; Pivovarov, G. I.; Lvova, N. A.; Gogolinsky, K.; Reshetov, V. *Diamond Relat. Mater*. **1998**, *7*, 427.

(15) Chernozatoskii, L. A.; Serebryanaya, N. R.; Mavrin, B. N. *Chem. Phys. Lett.* **2000**, *316*, 199.

(16) Serebryanaya, N. R.; Chernozatoskii, L. A. *Solid State Commun.* **2000**, *114*, 537.

(17) Yildirim, T.; Gülseren, O.; Kilic, C.; Ciraci, S. *Phys. Rev. B* **2000**, *62*, 12648.

(18) Chernozatonskii, L. A. *Chem. Phys. Lett.* **1998**, *297*, 257.

(19) Wood, J. R.; Frogley, M. D.; Meurs, E. R.; Prins, A. D.; Peijs, T.; Dunstan, D.; Wagner, H. D. *J. Phys. Chem. B* **1999**, *103*, 10388.

(20) Venkateswaran, U. D.; Rao, A. M.; Richter, E.; Menon, M.; Rinzler, A.; Smalley, R. E.; Eklund, P. C. *Phys. Rev. B* **1999**, 59, 10928.

(21) Teredesai, P. V.; Sood, A. K.; Muthu, D. V. S.; Sen, R.; Govindaraj, V.; Rao, C. N. R. *Chem. Phys. Lett.* **2000**, *319*, 296.

(22) Chesnokov, S. A.; Nalimova, V. A.; Rinzler, A. G.; Smalley, R. E.; Fischer, J. E. *Phys. Rev. Lett.* **1999**, *82*, 343.

(23) Tang, J.; Qin, L.-C.; Sasaki, T.; Yudasaka, M.; Matsushita, A.; Iijima, S. *Phys. Rev. Lett.* **2000**, *85*, 1887.

(24) Sharma, S. M.; Karmakar, S.; Sikka, S. K.; Teredesai, P. V.; Sood, A. K.; Govindaraj, V.; Rao, C. N. R. *Phys. Rev. B* **2001**, *63*, 205417.

(25) Gu, Z.; Brinson, B.; Zimmerman, J. L.; Khabashesku, V. N.; Margrave, J. L.; Davydov, V. A.; Kashevarova, L. S.; Rakhmanina, A. V.; Yakovlev, E. N. *NANOSPACE 2001: Exploring Interdisciplinary Frontiers. The International Conference on Integrated Nano/Microtechnology for Space and Biomedical Applications*; Galveston, TX, March 13−16, 2001; Abstr. p 218.

(26) Shukla, R.; Zimmerman, J. L.; Khabashesku, V. N.; Margrave, J. L.; Davydov, V. A.; Kashevarova, L. S.; Rakhmanina, A. V.; Yakovlev, E. N. *Rice Quantum Institute Fourteenth Annual Summer Research Colloquium*; Houston, TX, August 11, 2000; Abstr. p 21.

(27) Guo, T.; Nikolaev, P.; Thess, A.; Colbert, D. T.; Smalley, R. E. *Chem. Phys. Lett.* **1995**, *243*, 49.

(28) Thess, A.; Lee, R.; Nikolaev, P.; Dai, H. J.; Petit, J.; Robert, J.; Xu, C. H.; Lee, Y. H.; Kim, S. G.; Rinzler, A. G.; Colbert, D. T.; Scusseria, G. E.; Tomanek, D.; Foscher, J. E.; Smalley, R. E. *Science* **1996**, *273*, 483.

(29) Liu, J.; Rinzler, A. G.; Dai, H. J.; Hafner, J. H.; Bradley, R. K.; Boul, P. J.; Lu, A.; Iverson, T.; Shelimov, K.; Huffman, C. B.; Rodriguez-Macias, F. J.; Shon, Y. S.; Lee, T. R.; Colbert, D. T.; Smalley, R. E. *Science* **1998**, *280*, 1253.

(30) Rinzler, A. G.; Liu, J.; Dai, H.; Nikolaev, P.; Huffman, C. B.; Rodriguez-Macias, F. J.; Boul, P. J.; Lu, A. H.; Heymann, D.; Colbert, D. T.; Lee, R. S.; Fischer, J. E.; Rao, A. M.; Eklund, P. C.; Smalley, R. E. *Appl. Phys. A* **1998**, *67*, 29.

(31) Khvostantsev, L. G.; Vereschagin, L. F.; Novikov, A. P. *High Temp.-High Press*. **1977**, *9*, 637.

(32) Davydov, V. A.; Kashevarova, L. S.; Rakhmanina, A. V.; Agafonov, V.; Ceolin, R.; Szwarc, H. *Carbon* **1997**, *35*, 735.

(33) Rao, A. M.; Richter, E.; Bandow, S.; Eklund, P. C.; Williams, K. A.; Fang, S.; Subbaswamy, K. R.; Menon, M.; Thess, A.; Smalley, R. E.; Dresselhaus, G.; Dresselhaus, M. S. *Science* **1997**, *275*, 187.

(34) Chen, J.; Deng, S. Z.; Chen, J.; Yu, Z. X.; Xu, N. S. *Appl. Phys. Lett.* **1999,** *74*, 3651.

(35) Popov, M.; Kyotani, M.; Koga, Y.; Nemanich, R. J. *Proceedings of the Sixth Applied Diamond Conference/Second Frontier Carbon Technology Joint Conference (ADC/FCT 2001)*; Aug. 6−10, 2001, Auburn, AL; Tseng, Y., Miyoshi, K., Yoshikawa, M., Murakawa, M., Koga, Y., Kobashi, K., Amaratunga, G. A. J., Eds.; pp 681−685.

(36) Popov, M.; Kyotani, M.; Nemanich, R. J.; Koga, Y. *Phys. Rev. B* **2002**, *65*, 033408.